Interval-Arithmetic-Based Robust Control of Fully-Actuated Mechanical Systems

Andrea Giusti, Stefan B. Liu, and Matthias Althoff

***Abstract*—We propose a control approach for fully-actuated mechanical systems using interval arithmetic, which guarantees global uniform ultimate boundedness of the tracking error and robust performance despite model uncertainties and input disturbances. Existing robust control methods often require computationally expensive or empirical estimations of bounds of state-dependent, nonlinear perturbations, arising from model mismatches. Our robust feedback control approach is different and removes these difficulties by using interval arithmetic to determine online the worst-case perturbation acting on the error dynamics. We present two interval-arithmetic-based robust controllers by robustifying inverse-dynamics and passivity-based nominal control schemes. The effectiveness of our approach is demonstrated on a real robot manipulator with uncertain dynamics.**

***Index Terms*—Robust control, interval arithmetic, inverse-dynamics control, passivity-based control, mechanical systems, uncertain systems.**

I. Introduction

ROBUST control methods enhance the control performance of dynamical systems despite uncertainties and disturbances [1]. The mathematical models typically used for control design can only approximate the real system dynamics up to a certain degree. This can result in limited effectiveness or even in incorrect behavior when closed-loop control performance shall be guaranteed, e.g., in safety-critical [2], [3] or high performance scenarios [4], [5]. Violations of performance specifications often requires one to deploy new control laws or meticulously tune the current controller.

In this paper we consider the class of dynamical systems that can be described by the Euler-Lagrange formulation [6], are fully actuated, and have uncertain parameters. Widely adopted representatives of this system class are robot manipulators. The robust control problem of these systems has attracted numerous researchers. Effective classical and more recent approaches are well documented in textbooks, such as [7]–[10]. A survey that describes works until the early '90s can be found in [11] and more recent contributions are, e.g., [12]–[18]. Methods that are based on the optimal control framework for robust control have been presented, e.g., in [15], [16]. Sliding-mode controllers have been proposed for robust control of mechanical systems e.g., in [19], [20], with second-order variants to alleviate the chattering phenomenon [21], [22]. Robust control methods based on the online estimation of plant uncertainties and external disturbances by means of disturbance observers have been proposed in [23], [24], and a recent comprehensive survey of these approaches can be found in [25]. Recent methods combining principles of both adaptive and robust control techniques have been proposed in [26]–[28].

Previous robust control methods that guarantee asymptotic convergence of the tracking error result in discontinuous control laws [29]. However, control schemes with discontinuous control laws are difficult to implement in practice due to the induced chattering [30]. Chattering is highly undesired for mechanical systems since it often excites unmodeled high-frequency dynamics. The discontinuous robust control action can often be smoothed as presented in [31], where the authors introduce a practical stability notion for uncertain systems using the concept of uniform ultimate boundedness of the tracking error. The work in [12] adopts the smoothing concept for robot manipulators and exploits the property that their dynamics can be made linear in the dynamic coefficients composed of inertial parameters (see e.g., [9, Section 7.2.2]). There, the perturbations due to model uncertainty is directly determined by the dynamic coefficients, instead of considering bounds on highly nonlinear state-dependent perturbation functions with respect to other control approaches. The effectiveness of that approach has been experimentally evaluated in [32] on a directly-actuated planar robot with two degrees of freedom. Also the scheme in [33, Section 2.4.2], exploits the property of linearity in the dynamic coefficients for robot manipulators with an intrinsically continuous control law.

The a-priori estimation of bounds of perturbations that act on the closed-loop error dynamics, which many proposed robust control techniques require, is not simple to perform in practice since these bounds are composed of highly nonlinear state-dependent functions. They either require computationally expensive sampling approaches to sufficiently cover the reachable state space, or empirical estimations through testing; however, both approaches are not formally correct. In summary, most existing robust control schemes for mechanical systems either result in discontinuous control laws, e.g., [28], [29], require a priori estimation of bounds of nonlinear, state-dependant perturbation functions [14], [18], or require a particular linear factorization of the system dynamics [12], [13].

We propose an approach to resolve the above-mentioned difficulties for robust control of fully-actuated mechanical systems. Our proposed schemes result in continuous control laws that do not require any a-priori estimation of bounds of nonlinear state-dependent perturbation terms, nor any particular factorization of the system dynamics. In particular,

A. Giusti is with the Unit of Robotics and Intelligent Systems Engineering, Fraunhofer Italia Research, Bolzano, 39100, Italy, e-mail: andrea.giusti@fraunhofer.it.

S. Liu is with the Department of Informatics, Technical University of Munich (TUM), Garching, 85748, Germany, e-mail: stefan.liu@tum.de.

M. Althoff is with the Department of Informatics, Technical University of Munich (TUM), Garching, 85748, Germany, e-mail: matthias.althoff@tum.de.

Manuscript received Month DD, YYYY; revised Month DD, YYYY.

we propose using interval arithmetic for the automatic online computation of worst-case perturbations, and use this measure for computing a robustifying feedback control action. This has the additional benefit of providing formally-guaranteed over-approximative results. Previous work that considered designing robust control schemes for linear systems using interval arithmetic can be found in [34]–[37]. Our proposed robust control approach, however, does not require linearity. This paper is an extension of our previous work in [38] and presents additional theoretical results and experiments on a six degrees-of-freedom robot arm. We have also applied our approach to a simulated continuum robot in [39].

The remainder of the paper is structured as follows. In Section II we provide preliminaries on interval arithmetic and we detail the control problem. Our proposed control approach is presented in Section III. Experimental results are presented in Section IV, and the conclusions in Section V.

II. Problem Statement

In this section, we first introduce preliminaries on interval arithmetic followed by describing the addressed control problem.

A. Preliminaries on Interval Arithmetic

Interval arithmetic [40] allows one to bound solutions of mathematical problems involving uncertain parameters with certainty. For subsequent derivations, the following definitions are introduced.

Definition 1 (Multidimensional interval): A multidimensional interval is defined as a set of real numbers:

$$[\mathbf{x}] := [\underline{\mathbf{x}}, \overline{\mathbf{x}}], \quad \underline{\mathbf{x}} \in \mathbb{R}^n, \ \overline{\mathbf{x}} \in \mathbb{R}^n, \ \underline{x_i} \leq \overline{x}_i, \ \forall \ i \in \{1, \ldots, n\}.$$

The scalar case is simply denoted by $[x]$ instead of $[\mathbf{x}]$, with $\underline{x}$ for denoting its infimum and $\overline{x}$ its supremum.

Definition 2 (Interval-valued function): An interval-valued function can be seen as an extension of a real-valued function evaluated for one or more interval arguments. More precisely, given a generic real-valued function $\mathbf{w} : \mathbb{R}^n \to \mathbb{R}^m$, its interval evaluation over a set $[\mathbf{x}]$ is defined as

$$\mathbf{w}([\mathbf{x}]) := \{\mathbf{w}(\mathbf{x}) \mid \mathbf{x} \in [\mathbf{x}]\}.$$

Operations among interval variables, vectors and matrices, also known as set-based operations, can be implemented, e.g., as in [41], [42].

B. Control Problem

We consider uncertain, fully-actuated mechanical systems whose dynamics can be modeled by the Lagrangian formulation (see e.g., [10, Section 6.1]). Subsequently, we omit time dependence for brevity when this does not affect the clarity of the description. After introducing a vector $\boldsymbol{\Delta} \in \mathbb{R}^M$ of M model parameters and a vector $\mathbf{q} \in \mathbb{R}^N$ of N generalized coordinates, we can compactly write the model of the system dynamics as:

$$\mathbf{M}(\mathbf{q}, \boldsymbol{\Delta})\ddot{\mathbf{q}} + \overbrace{\mathbf{C}(\mathbf{q}, \dot{\mathbf{q}}, \boldsymbol{\Delta})\dot{\mathbf{q}} + \mathbf{f}(\dot{\mathbf{q}}, \boldsymbol{\Delta}) + \mathbf{g}(\mathbf{q}, \boldsymbol{\Delta})}^{:= \mathbf{n}(\mathbf{q}, \dot{\mathbf{q}}, \boldsymbol{\Delta})} = \mathbf{u} + \mathbf{d}, \qquad (1)$$

where $\mathbf{M}(\mathbf{q}, \boldsymbol{\Delta}) \in \mathbb{R}^{N \times N}$ is the symmetric positive definite inertia matrix, $\mathbf{C}(\mathbf{q}, \dot{\mathbf{q}}, \boldsymbol{\Delta})\dot{\mathbf{q}}$ is the vector containing the Coriolis and centrifugal model terms, and $\mathbf{f}(\dot{\mathbf{q}}, \boldsymbol{\Delta})$ and $\mathbf{g}(\mathbf{q}, \boldsymbol{\Delta})$ are the vectors of friction and gravity terms, respectively. Further, $\mathbf{d} \in \mathbb{R}^N$ is a disturbance input and $\mathbf{u} \in \mathbb{R}^N$ is an actuation input which allows us to independently set commands for each generalized coordinate resulting in a fully-actuated system. Additionally, $\mathbf{C}(\mathbf{q}, \dot{\mathbf{q}}, \boldsymbol{\Delta}) \in \mathbb{R}^{N \times N}$ is a matrix such that the following property holds [6, Chapter 2]:

$$\mathbf{x}^T \left(\dot{\mathbf{M}}(\mathbf{q}, \boldsymbol{\Delta}) - 2\,\mathbf{C}(\mathbf{q}, \dot{\mathbf{q}}, \boldsymbol{\Delta}) \right) \mathbf{x} = \mathbf{0}, \quad \forall \mathbf{x} \in \mathbb{R}^N. \qquad (2)$$

We also consider that the following property holds [6, Chapter 2]:

$$\lambda_m \|\mathbf{x}\|^2 \leq \mathbf{x}^T \mathbf{M}(\mathbf{q}, \boldsymbol{\Delta})\mathbf{x} \leq \lambda_M \|\mathbf{x}\|^2, \ \forall \mathbf{x} \in \mathbb{R}^N, \qquad (3)$$

where $\lambda_m = \lambda_{min}(\mathbf{M}(\mathbf{q}, \boldsymbol{\Delta})) > 0$ and $\lambda_M = \lambda_{max}(\mathbf{M}(\mathbf{q}, \boldsymbol{\Delta})) < \infty$ are the minimum and maximum eigenvalues of the matrix $\mathbf{M}(\mathbf{q}, \boldsymbol{\Delta})$, respectively. We assume that:

1) the uncertainty of the model parameters is known and bounded by the multidimensional interval $[\boldsymbol{\Delta}]$: $\boldsymbol{\Delta} \in [\boldsymbol{\Delta}]$;
2) a vector of nominal model parameters $\boldsymbol{\Delta}_0 \in [\boldsymbol{\Delta}]$ is available;
3) the norm of the disturbance input vector $\mathbf{d}$ is bounded[1] by β_d (we consider both cases for this scalar to be known or not);
4) the terms in (1) are continuous $\forall \mathbf{q}, \dot{\mathbf{q}} \in \mathbb{R}^N$, and Lipschitz continuous for $\boldsymbol{\Delta} \in [\boldsymbol{\Delta}]$ with given values of $\mathbf{q}$, $\dot{\mathbf{q}}$.

For the considered systems and assumptions we face the problem of designing controllers that guarantee both global uniform ultimate boundedness [43, Section 4.8] of the tracking error and robust performance, despite parametric model uncertainties and input disturbances. In particular, by considering the control error $\mathbf{e}(t) = \mathbf{q}_d(t) - \mathbf{q}(t)$, we address the problem of formally ensuring that

$$\|\mathbf{e}(t)\| < \varepsilon, \ \forall \, t \geq t_1,$$

for a finite time $t_1 \geq 0$, a finite $\varepsilon > 0$ and reference trajectories $\mathbf{q}_d(t)$ that are sufficiently smooth (at least twice differentiable). We denote this result as robust performance if ε is defined by the user a priori. If ε is not defined by the user a priori, we use the term Global Uniform Ultimate Boundedness of the tracking error (GUUB).

III. Interval-Arithmetic-Based Robust Control

We introduce two variants of interval-arithmetic-based robust controllers differing in the nominal tracking control law. First, the case of using inverse-dynamics nominal control is described in Subsection III-A, followed by the case of using passivity-based nominal control in Subsection III-B. These two schemes will be denoted by Interval-Arithmetic Inverse-Dynamics (IA-ID) control and Interval-Arithmetic Passivity-Based (IA-PB) control. For compactness of the following description, the model terms computed with nominal model parameters $\boldsymbol{\Delta}_0$ are denoted with 0 as a subscript. For example, the nominal inertia matrix $\mathbf{M}(\mathbf{q}, \boldsymbol{\Delta}_0)$ will be simply denoted

[1] All norms in this work are 2-norms.

by $\mathbf{M}_0(\mathbf{q})$. Furthermore, we use a tilde to denote the mismatch between nominal and the real model terms. For example, we denote the model mismatch of the inertia matrix as

$$\tilde{\mathbf{M}}(\mathbf{q},\boldsymbol{\Delta}) = \mathbf{M}(\mathbf{q},\boldsymbol{\Delta}) - \mathbf{M}_0(\mathbf{q}).$$

A. Interval-Arithmetic Inverse-Dynamics Control

In this subsection, we derive the IA-ID controller for ensuring GUUB, assuming β_d to be known. Let us consider the standard inverse-dynamics control law [9, Section 8.5.2], with an auxiliary input vector $\boldsymbol{\nu}_{ID} \in \mathbb{R}^N$ as

$$\mathbf{u} = \mathbf{M}_0(\mathbf{q})\mathbf{y} + \overbrace{\mathbf{C}_0(\mathbf{q},\dot{\mathbf{q}})\dot{\mathbf{q}} + \mathbf{f}_0(\dot{\mathbf{q}}) + \mathbf{g}_0(\mathbf{q})}^{:=\mathbf{n}_0(\mathbf{q},\dot{\mathbf{q}})} - \boldsymbol{\nu}_{ID}, \quad (4)$$

where

$$\mathbf{y} = \ddot{\mathbf{q}}_d + \mathbf{K}_D\dot{\mathbf{e}} + \mathbf{K}_P\mathbf{e},$$

with $\mathbf{K}_P$ and $\mathbf{K}_D$ being positive definite matrices of proper dimensions and where $\mathbf{n}_0$ contains the nominal contributions due to centrifugal, Coriolis, friction, and gravity terms. By applying (4) in (1), we obtain

$$\mathbf{M}(\mathbf{q},\boldsymbol{\Delta})\ddot{\mathbf{q}} = \mathbf{M}_0(\mathbf{q})\mathbf{y} + \mathbf{n}_0(\mathbf{q},\dot{\mathbf{q}}) - \mathbf{n}(\mathbf{q},\dot{\mathbf{q}},\boldsymbol{\Delta}) - \boldsymbol{\nu}_{ID} + \mathbf{d}. \quad (5)$$

Subtracting the term $\mathbf{M}(\mathbf{q},\boldsymbol{\Delta})(\ddot{\mathbf{q}}_d + \mathbf{K}_D\dot{\mathbf{e}} + \mathbf{K}_P\mathbf{e})$ from both sides of (5) yields

$$\mathbf{M}(\mathbf{q},\boldsymbol{\Delta})(\ddot{\mathbf{e}} + \mathbf{K}_D\dot{\mathbf{e}} + \mathbf{K}_P\mathbf{e}) = \mathbf{w}_{ID}(\mathbf{q},\dot{\mathbf{q}},\mathbf{y},\boldsymbol{\Delta}_0,\boldsymbol{\Delta},\mathbf{d}) + \boldsymbol{\nu}_{ID}, \quad (6)$$

where

$$\mathbf{w}_{ID}(\mathbf{q},\dot{\mathbf{q}},\mathbf{y},\boldsymbol{\Delta}_0,\boldsymbol{\Delta},\mathbf{d}) = \tilde{\mathbf{M}}(\mathbf{q},\boldsymbol{\Delta})\mathbf{y} + \tilde{\mathbf{n}}(\mathbf{q},\dot{\mathbf{q}},\boldsymbol{\Delta}) - \mathbf{d} \quad (7)$$

is the perturbation arising from model mismatches and external disturbances.

The interval-arithmetic robust control action can now be introduced through $\boldsymbol{\nu}_{ID}$. We first define a measure of the worst-case perturbation as

$$\boldsymbol{\rho}([\boldsymbol{\Phi}_{ID}]) = \max\left(|\underline{\boldsymbol{\Phi}}_{ID}|, |\overline{\boldsymbol{\Phi}}_{ID}|\right), \quad (8)$$

in which the max operator is applied element-wise and where[2]

$$[\boldsymbol{\Phi}_{ID}] = \mathbf{w}_{ID}(\mathbf{q},\dot{\mathbf{q}},\mathbf{y},\boldsymbol{\Delta}_0,[\boldsymbol{\Delta}],[\mathbf{d}]).$$

From Definition 2 it follows that

$$\mathbf{w}_{ID}(\mathbf{q},\dot{\mathbf{q}},\mathbf{y},\boldsymbol{\Delta}_0,\boldsymbol{\Delta},\mathbf{d}) \in [\boldsymbol{\Phi}_{ID}] = \mathbf{w}_{ID}(\mathbf{q},\dot{\mathbf{q}},\mathbf{y},\boldsymbol{\Delta}_0,[\boldsymbol{\Delta}],[\mathbf{d}]),$$

and consequently

$$\rho_i([\boldsymbol{\Phi}_{ID}]) \geq |w_{ID,i}(\mathbf{q},\dot{\mathbf{q}},\mathbf{y},\boldsymbol{\Delta}_0,\boldsymbol{\Delta},\mathbf{d})|, \quad (9)$$
$$\forall\, \mathbf{q},\, \dot{\mathbf{q}},\, \mathbf{y} \in \mathbb{R}^N,\, \boldsymbol{\Delta}_0 \in [\boldsymbol{\Delta}] \text{ and } \boldsymbol{\Delta} \in [\boldsymbol{\Delta}],\, \mathbf{d} \in [\mathbf{d}].$$

Next, we use $\boldsymbol{\rho}([\boldsymbol{\Phi}_{ID}])$ for feedback control. From (6), the closed-loop error-dynamics

$$\dot{\boldsymbol{\xi}} = \mathbf{A}\boldsymbol{\xi} + \mathbf{B}\mathbf{M}^{-1}\boldsymbol{\nu}_{ID} + \mathbf{B}\mathbf{M}^{-1}\mathbf{w}_{ID}, \quad (10)$$

can be obtained, where

$$\boldsymbol{\xi} = (\mathbf{e}^T,\ \dot{\mathbf{e}}^T)^T, \quad (11)$$

$$\mathbf{A} = \begin{pmatrix} \mathbf{0} & \mathbf{I} \\ -\mathbf{K}_P & -\mathbf{K}_D \end{pmatrix},\quad \mathbf{B} = \begin{pmatrix} \mathbf{0} \\ \mathbf{I} \end{pmatrix}. \quad (12)$$

The following derivation relies on similar arguments as in [33, Section 2.4.2] extended by methods from interval arithmetic. By considering a symmetric positive definite matrix $\mathbf{P}$ such that

$$\mathbf{A}^T\mathbf{P} + \mathbf{P}\mathbf{A} = -\mathbf{Q} \quad (13)$$

with $\mathbf{Q}$ being positive definite, we use the Lyapunov function candidate

$$\mathbf{V} = \boldsymbol{\xi}^T\mathbf{P}\boldsymbol{\xi}. \quad (14)$$

The derivative with respect to time of (14) along the solution of (10) yields

$$\begin{aligned}\dot{\mathbf{V}} &= -\boldsymbol{\xi}^T\mathbf{Q}\boldsymbol{\xi} + 2\boldsymbol{\xi}^T\mathbf{P}\mathbf{B}\mathbf{M}^{-1}\left(\boldsymbol{\nu}_{ID} + \mathbf{w}_{ID}\right) \\ &\overset{(9)}{\leq} -\boldsymbol{\xi}^T\mathbf{Q}\boldsymbol{\xi} + 2\boldsymbol{\xi}^T\mathbf{P}\mathbf{B}\mathbf{M}^{-1}\boldsymbol{\nu}_{ID} + \\ &\quad 2\|\boldsymbol{\xi}^T\mathbf{P}\mathbf{B}\|\|\mathbf{M}^{-1}\|\|\boldsymbol{\rho}\left([\boldsymbol{\Phi}_{ID}]\right)\|. \end{aligned} \quad (15)$$

By considering that $\lambda_{min}(\mathbf{M}^{-1}) = \frac{1}{\lambda_{max}(\mathbf{M})}$, $\lambda_{max}(\mathbf{M}^{-1}) = \frac{1}{\lambda_{min}(\mathbf{M})}$, and using (3), we have that

$$\frac{1}{\lambda_M}\|\mathbf{x}\|^2 \leq \mathbf{x}^T\mathbf{M}^{-1}(\mathbf{q},\boldsymbol{\Delta})\mathbf{x} \leq \frac{1}{\lambda_m}\|\mathbf{x}\|^2 \quad \forall\, \mathbf{x} \in \mathbb{R}^N, \quad (16)$$

and by selecting the robustifying term of the controller as

$$\boldsymbol{\nu}_{ID} = -\kappa_P\|\boldsymbol{\rho}\left([\boldsymbol{\Phi}_{ID}]\right)\|^2\mathbf{B}^T\mathbf{P}\boldsymbol{\xi}, \quad (17)$$

where $\kappa_P > 0$ is a tuning parameter, (15) becomes

$$\begin{aligned}\dot{\mathbf{V}} &\leq -\boldsymbol{\xi}^T\mathbf{Q}\boldsymbol{\xi} - 2\,\kappa_P\|\boldsymbol{\rho}\left([\boldsymbol{\Phi}_{ID}]\right)\|^2\boldsymbol{\xi}^T\mathbf{P}\mathbf{B}\mathbf{M}^{-1}\mathbf{B}^T\mathbf{P}\boldsymbol{\xi} + \\ &\quad 2\|\boldsymbol{\xi}^T\mathbf{P}\mathbf{B}\|\|\mathbf{M}^{-1}\|\|\boldsymbol{\rho}\left([\boldsymbol{\Phi}_{ID}]\right)\| \\ &\overset{(16)}{\leq} -\boldsymbol{\xi}^T\mathbf{Q}\boldsymbol{\xi} - \frac{2\kappa_P}{\lambda_M}\|\boldsymbol{\xi}^T\mathbf{P}\mathbf{B}\|^2\|\boldsymbol{\rho}\left([\boldsymbol{\Phi}_{ID}]\right)\|^2 + \\ &\quad \frac{2}{\lambda_m}\|\boldsymbol{\xi}^T\mathbf{P}\mathbf{B}\|\|\boldsymbol{\rho}\left([\boldsymbol{\Phi}_{ID}]\right)\| \\ &\leq -\boldsymbol{\xi}^T\mathbf{Q}\boldsymbol{\xi} + \\ &\quad \frac{2\kappa_P}{\lambda_M}\|\boldsymbol{\xi}^T\mathbf{P}\mathbf{B}\|\|\boldsymbol{\rho}\left([\boldsymbol{\Phi}_{ID}]\right)\|\left(\frac{\lambda_M}{\kappa_P\lambda_m} - \|\boldsymbol{\xi}^T\mathbf{P}\mathbf{B}\|\|\boldsymbol{\rho}\left([\boldsymbol{\Phi}_{ID}]\right)\|\right). \end{aligned} \quad (18)$$

It is now possible to observe from (18) that when $\|\boldsymbol{\xi}^T\mathbf{P}\mathbf{B}\|\|\boldsymbol{\rho}\left([\boldsymbol{\Phi}_{ID}]\right)\| \geq \frac{\lambda_M}{\kappa_P\lambda_m}$, then $\dot{\mathbf{V}} \leq -\boldsymbol{\xi}^T\mathbf{Q}\boldsymbol{\xi}$, while for $\|\boldsymbol{\xi}^T\mathbf{P}\mathbf{B}\|\|\boldsymbol{\rho}\left([\boldsymbol{\Phi}_{ID}]\right)\| < \frac{\lambda_M}{\kappa_P\lambda_m}$ we can write that

$$\begin{aligned}\dot{\mathbf{V}} &\leq -\boldsymbol{\xi}^T\mathbf{Q}\boldsymbol{\xi} + \frac{2}{\lambda_m}\|\boldsymbol{\xi}^T\mathbf{P}\mathbf{B}\|\|\boldsymbol{\rho}\left([\boldsymbol{\Phi}_{ID}]\right)\| \\ &\leq -\lambda_{\min}(\mathbf{Q})\|\boldsymbol{\xi}\|^2 + \frac{2\lambda_M}{\kappa_P\lambda_m^2}. \end{aligned}$$

In light of this result, GUUB follows from [43, Theorem 4.18]. From this, it also follows that the designer can increase tracking performance by increasing κ_P. The block diagram of the IA-ID controller is presented in Figure 1.

Remark 1: An important aspect of (17) is that it is continuous. Continuity follows from the fact that (8) is continuous. In particular, given that $[\boldsymbol{\Phi}_{ID}] = \mathbf{w}_{ID}(\mathbf{q},\dot{\mathbf{q}},\mathbf{y},\boldsymbol{\Delta}_0,[\boldsymbol{\Delta}],[\mathbf{d}])$, for given $\mathbf{q}$, $\dot{\mathbf{q}}$, $\mathbf{y}$, $\boldsymbol{\Delta}_0$, one can choose $\mathbf{d}^* \in [\mathbf{d}]$ and $\boldsymbol{\Delta}^* \in [\boldsymbol{\Delta}]$ such that $\overline{\boldsymbol{\Phi}}_{ID}$ is maximal (or $\underline{\boldsymbol{\Phi}}_{ID}$ is minimal). Since $\mathbf{w}_{ID}(\mathbf{q},\dot{\mathbf{q}},\mathbf{y},\boldsymbol{\Delta}_0,\boldsymbol{\Delta}^*,\mathbf{d}^*)$ is continuous, it guarantees in turn continuity of $|\overline{\boldsymbol{\Phi}}_{ID}|$ (or $|\underline{\boldsymbol{\Phi}}_{ID}|$). Then, since the max operator between two continuous functions preserves continuity, $\boldsymbol{\rho}([\boldsymbol{\Phi}_{ID}])$ is continuous.

[2]The dependencies of $[\boldsymbol{\Phi}_{ID}]$ from $\mathbf{q}$, $\dot{\mathbf{q}}$, $\mathbf{y}$, and $\boldsymbol{\Delta}_0$ are omitted for brevity.

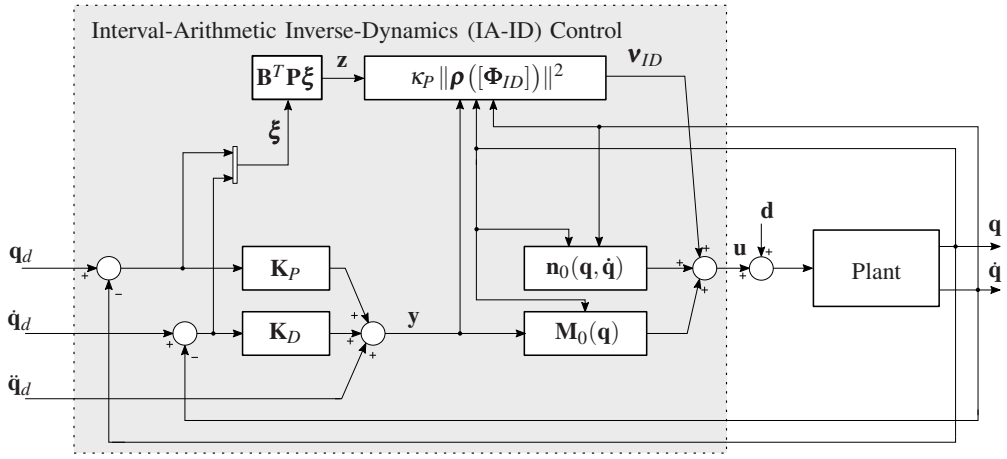

Fig. 1. Block diagram of Interval-Arithmetic Inverse-Dynamics (IA-ID) control.

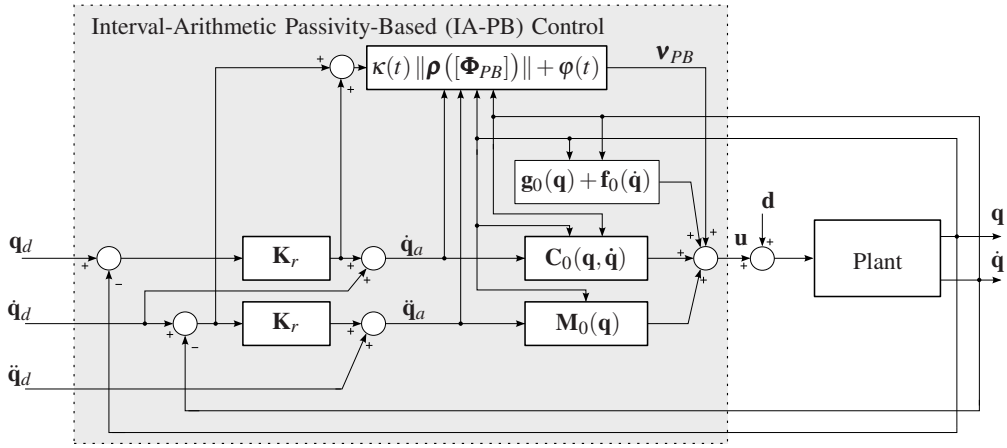

Fig. 2. Block diagram of Interval-Arithmetic Passivity-Based (IA-PB) control.

B. Interval-Arithmetic Passivity-Based Control

In this subsection, we first derive the IA-PB controller for ensuring GUUB, considering known bounds β_d of the external disturbance vector $\mathbf{d}$. Subsequently, we enhance this scheme to achieve robust performance. In this second description we also relax the assumption that β_d is known.

1) GUUB with IA-PB control: Let us consider the following nominal passivity-based control scheme [33] with the auxiliary input vector $\boldsymbol{\nu}_{PB}$ as:

$$\mathbf{u} = \mathbf{M}_0(\mathbf{q})\ddot{\mathbf{q}}_a + \mathbf{C}_0(\mathbf{q},\dot{\mathbf{q}})\dot{\mathbf{q}}_a + \mathbf{f}_0(\dot{\mathbf{q}}) + \mathbf{g}_0(\mathbf{q}) - \boldsymbol{\nu}_{PB}, \tag{19}$$

with

$$\dot{\mathbf{q}}_a = \dot{\mathbf{q}}_d + \mathbf{K}_r\mathbf{e} \tag{20}$$

and $\mathbf{K}_r$ being a diagonal positive definite matrix of proper dimensions. By inserting the control law (19) in (1) we obtain

$$\mathbf{M}(\mathbf{q},\Delta)\dot{\mathbf{r}} + \mathbf{C}(\mathbf{q},\dot{\mathbf{q}},\Delta)\mathbf{r} = \boldsymbol{\nu}_{PB} + \mathbf{w}_{PB}(\mathbf{q},\dot{\mathbf{q}},\dot{\mathbf{q}}_a,\ddot{\mathbf{q}}_a,\boldsymbol{\Delta}_0,\boldsymbol{\Delta},\mathbf{d}), \tag{21}$$

where

$$\mathbf{r} = \dot{\mathbf{e}} + \mathbf{K}_r\mathbf{e}, \tag{22}$$

and

$$\mathbf{w}_{PB}(\mathbf{q},\dot{\mathbf{q}},\dot{\mathbf{q}}_a,\ddot{\mathbf{q}}_a,\boldsymbol{\Delta}_0,\boldsymbol{\Delta},\mathbf{d}) = \tilde{\mathbf{M}}(\mathbf{q},\Delta)\ddot{\mathbf{q}}_a + \tilde{\mathbf{C}}(\mathbf{q},\dot{\mathbf{q}},\Delta)\dot{\mathbf{q}}_a + \tilde{\mathbf{f}}(\dot{\mathbf{q}},\Delta) + \tilde{\mathbf{g}}(\mathbf{q},\Delta) - \mathbf{d}. \tag{23}$$

As previously done for IA-ID, the following relation can be written[3]:

$$[\boldsymbol{\Phi}_{PB}] = \mathbf{w}_{PB}(\mathbf{q},\dot{\mathbf{q}},\dot{\mathbf{q}}_a,\ddot{\mathbf{q}}_a,\boldsymbol{\Delta}_0,[\boldsymbol{\Delta}],[\mathbf{d}]),$$

$$\mathbf{w}_{PB}(\mathbf{q},\dot{\mathbf{q}},\dot{\mathbf{q}}_a,\ddot{\mathbf{q}}_a,\boldsymbol{\Delta}_0,\boldsymbol{\Delta},\mathbf{d}) \in [\boldsymbol{\Phi}_{PB}], \tag{24}$$

where the set-membership relation of (24) follows from Definition 2. The worst-case perturbation is

$$\boldsymbol{\rho}([\boldsymbol{\Phi}_{PB}]) = \max\left(|\underline{\boldsymbol{\Phi}}_{PB}|, |\overline{\boldsymbol{\Phi}}_{PB}|\right). \tag{25}$$

From the same arguments as for the inverse-dynamics variant, it holds that

$$\rho_i([\boldsymbol{\Phi}_{PB}]) \geq |w_{PB,i}(\mathbf{q},\dot{\mathbf{q}},\dot{\mathbf{q}}_a,\ddot{\mathbf{q}}_a,\boldsymbol{\Delta}_0,\boldsymbol{\Delta},\mathbf{d})|, \tag{26}$$
$$\forall\, \mathbf{q},\, \dot{\mathbf{q}},\, \dot{\mathbf{q}}_a,\, \ddot{\mathbf{q}}_a, \in \mathbb{R}^N\, \boldsymbol{\Delta}_0 \in [\boldsymbol{\Delta}] \text{ and } \boldsymbol{\Delta} \in [\boldsymbol{\Delta}], \mathbf{d} \in [\mathbf{d}].$$

[3]The dependencies of $[\boldsymbol{\Phi}_{PB}]$ from $\mathbf{q}$, $\dot{\mathbf{q}}$, $\dot{\mathbf{q}}_a$, $\ddot{\mathbf{q}}_a$, and $\boldsymbol{\Delta}_0$ are omitted for brevity.

To derive the control law, it is convenient to start from the storage function

$$V(\mathbf{r}) = \frac{1}{2}\mathbf{r}^T\mathbf{M}(\mathbf{q},\Delta)\mathbf{r}, \tag{27}$$

whose derivative along the solution of (21) is

$$\begin{aligned}\dot{V}(\mathbf{r}) &= \mathbf{r}^T\mathbf{M}(\mathbf{q},\Delta)\dot{\mathbf{r}} + \frac{1}{2}\mathbf{r}^T\dot{\mathbf{M}}(\mathbf{q},\Delta)\mathbf{r} \\ &\overset{(21),(2)}{=} \mathbf{r}^T\boldsymbol{\nu}_{PB} + \mathbf{r}^T\mathbf{w}_{PB}(\mathbf{q},\dot{\mathbf{q}},\dot{\mathbf{q}}_a,\ddot{\mathbf{q}}_a,\boldsymbol{\Delta}_0,\boldsymbol{\Delta},\mathbf{d}).\end{aligned} \tag{28}$$

Using this result, the term $\boldsymbol{\nu}_{PB}$ is selected as

$$\boldsymbol{\nu}_{PB} = -\Big(\kappa_P\,\|\boldsymbol{\rho}\left([\boldsymbol{\Phi}_{PB}]\right)\| + \varphi_P\Big)\,\mathbf{r}, \tag{29}$$

with $\kappa_P \geq 1$ and $\varphi_P \geq 1$. Inserting this choice in (28) yields

$$\begin{aligned}\dot{V}(\mathbf{r}) &= -\varphi_P\,\|\mathbf{r}\|^2 - \kappa_P\,\|\boldsymbol{\rho}\left([\boldsymbol{\Phi}_{PB}]\right)\|\,\|\mathbf{r}\|^2 + \\ &\qquad \mathbf{r}^T\mathbf{w}_{PB}(\mathbf{q},\dot{\mathbf{q}},\dot{\mathbf{q}}_a,\ddot{\mathbf{q}}_a,\boldsymbol{\Delta}_0,\boldsymbol{\Delta},\mathbf{d}) \\ &\leq -\varphi_P\,\|\mathbf{r}\|^2 - \kappa_P\,\|\boldsymbol{\rho}\left([\boldsymbol{\Phi}_{PB}]\right)\|\,\|\mathbf{r}\|^2 + \\ &\qquad \|\mathbf{r}\|\,\|\mathbf{w}_{PB}(\mathbf{q},\dot{\mathbf{q}},\dot{\mathbf{q}}_a,\ddot{\mathbf{q}}_a,\boldsymbol{\Delta}_0,\boldsymbol{\Delta},\mathbf{d})\| \\ &\overset{(26)}{\leq} -\varphi_P\,\|\mathbf{r}\|^2 \underbrace{-\kappa_P\|\boldsymbol{\rho}\left([\boldsymbol{\Phi}_{PB}]\right)\|\,\|\mathbf{r}\|^2 + \|\mathbf{r}\|\|\boldsymbol{\rho}\left([\boldsymbol{\Phi}_{PB}]\right)\|}_{=:h_1(\mathbf{r})}.\end{aligned}$$

By factoring out $\|\mathbf{r}\|$ in $h_1(\mathbf{r})$, it follows that for $\|\mathbf{r}\| \geq \frac{1}{\kappa_P}$, $\dot{V}(\mathbf{r}) < 0$ since $h_1(\mathbf{r}) \leq 0$. From this result, GUUB is achieved as shown in [38, Theorem 1], which allows us to conclude that the trajectories $\mathbf{r}$ are ultimately bounded by

$$\|\mathbf{r}\| \leq \frac{1}{\kappa_P}\sqrt{\frac{\lambda_M}{\lambda_m}}.$$

The boundedness of the trajectories $\mathbf{r}$ implies boundedness of the tracking tracking error $\mathbf{e}$ as well, when $\mathbf{K}_r$ is properly chosen. This can be seen by considering the system in (22), with $\mathbf{r}$ as its bounded input. In fact, with $\mathbf{K}_r$ being diagonal and positive definite, this system is a set of first-order linear systems that asymptotically reach $|e_i| \leq \frac{|r_i|}{K_{r,i}}$ for each coordinate i. From this, it follows that the overall controller can ultimately reach any desired tracking performance with the selection of large enough gains of the matrix $\mathbf{K}_r$ and κ_P.

2) Robust performance with IA-PB control: By modifying $\boldsymbol{\nu}_{PB}$, a controller that can guarantee robust performance can also be obtained. In particular, this is possible without the need for finding large enough gains of $\mathbf{K}_r$ and the knowledge of λ_M, λ_m. Further, we now remove the assumption of knowing the bound β_d. The robust control action is now

$$\boldsymbol{\nu}_{PB} = -\Big(\kappa(t)\,\|\boldsymbol{\rho}\left([\boldsymbol{\Phi}_{PB}]\right)\| + \varphi(t)\Big)\,\mathbf{r}, \tag{30}$$

where $\kappa(t)$ and $\varphi(t)$ are two positive increasing functions with κ_P and φ_P as their respective minimum.

Given that the bound of the external disturbance vector norm is not known, it cannot be included in $\boldsymbol{\rho}([\boldsymbol{\Phi}_{PB}])$. Considering (28) and noticing that $\mathbf{w}_{PB}(\mathbf{q},\dot{\mathbf{q}},\dot{\mathbf{q}}_a,\ddot{\mathbf{q}}_a,\boldsymbol{\Delta}_0,\boldsymbol{\Delta},\mathbf{d}) = \mathbf{w}_{PB}(\mathbf{q},\dot{\mathbf{q}},\dot{\mathbf{q}}_a,\ddot{\mathbf{q}}_a,\boldsymbol{\Delta}_0,\boldsymbol{\Delta},\mathbf{0}) - \mathbf{d}$, the derivative of (27) can now be written as:

$$\begin{aligned}\dot{V}(\mathbf{r}) &= -\varphi(t)\,\|\mathbf{r}\|^2 - \kappa(t)\,\|\boldsymbol{\rho}\left([\boldsymbol{\Phi}_{PB}]\right)\|\,\|\mathbf{r}\|^2 + \\ &\qquad \mathbf{r}^T\mathbf{w}_{PB}(\mathbf{q},\dot{\mathbf{q}},\dot{\mathbf{q}}_a,\ddot{\mathbf{q}}_a,\boldsymbol{\Delta}_0,\boldsymbol{\Delta},\mathbf{0}) - \mathbf{r}^T\mathbf{d} \\ &\leq -\varphi(t)\,\|\mathbf{r}\|^2 - \kappa(t)\,\|\boldsymbol{\rho}\left([\boldsymbol{\Phi}_{PB}]\right)\|\,\|\mathbf{r}\|^2 + \\ &\qquad \|\mathbf{r}\|\,\|\mathbf{w}_{PB}(\mathbf{q},\dot{\mathbf{q}},\dot{\mathbf{q}}_a,\ddot{\mathbf{q}}_a,\boldsymbol{\Delta}_0,\boldsymbol{\Delta},\mathbf{0})\| + \|\mathbf{r}\|\beta_d \\ &\overset{(26)}{\leq} -\varphi(t)\,(1-\delta)\,\|\mathbf{r}\|^2 + h_2(\mathbf{r}),\end{aligned} \tag{31}$$

where

$$\begin{aligned}h_2(\mathbf{r}) = -\Big(\varphi(t)\,\delta + \kappa(t)\|\boldsymbol{\rho}\left([\boldsymbol{\Phi}_{PB}]\right)\|\Big)\|\mathbf{r}\|^2 + \\ \Big(\|\boldsymbol{\rho}\left([\boldsymbol{\Phi}_{PB}]\right)\| + \beta_d\Big)\,\|\mathbf{r}\|,\end{aligned}$$

and δ being a scalar such that $0 < \delta < 1$. By factoring out $\|\mathbf{r}\|$ in $h_2(\mathbf{r})$, it is not difficult to see that $h_2(\mathbf{r}) \leq 0$ for

$$\|\mathbf{r}\| \geq \frac{\|\boldsymbol{\rho}\left([\boldsymbol{\Phi}_{PB}]\right)\| + \beta_d}{\varphi(t)\,\delta + \kappa(t)\|\boldsymbol{\rho}\left([\boldsymbol{\Phi}_{PB}]\right)\|}. \tag{32}$$

From the right-hand side of (32), the following inequalities can be written:

$$\begin{aligned}\forall t:\ \frac{\|\boldsymbol{\rho}\left([\boldsymbol{\Phi}_{PB}]\right)\| + \beta_d}{\varphi(t)\,\delta + \kappa(t)\|\boldsymbol{\rho}\left([\boldsymbol{\Phi}_{PB}]\right)\|} &\leq \max\Big(\frac{\beta_d}{\varphi(t)\,\delta}, \frac{1}{\kappa(t)}\Big) \\ &\leq \max\Big(\frac{\beta_d}{\varphi_P\,\delta}, \frac{1}{\kappa_P}\Big).\end{aligned}$$

Assuming that β_d is finite, ultimate uniform boundedness of $\mathbf{r}$ follows from the same arguments used previously. In particular, the trajectories are ultimately bounded by

$$\|\mathbf{r}\| \leq \max\Big(\frac{\beta_d}{\varphi_P\,\delta}, \frac{1}{\kappa_P}\Big)\sqrt{\frac{\lambda_M}{\lambda_m}}. \tag{33}$$

By properly choosing the functions $\varphi(t)$ and $\kappa(t)$, this control scheme can also guarantee that a user-defined tracking performance is ultimately met, thus guaranteeing robust performance. In fact, with the use of the complete feedback control law composed of (19), (30), and

$$\begin{aligned}\varphi(t) &= \Big(\varphi_P + \varphi_I\int_0^t f(\|\mathbf{e}\|)\,d\tau\Big), \\ \kappa(t) &= \Big(\kappa_P + \kappa_I\int_0^t f(\|\mathbf{e}\|)\,d\tau\Big),\end{aligned}$$

where κ_I, $\varphi_I > 0$, $\mathbf{K}_r$ diagonal and positive definite, and

$$f(\|\mathbf{e}\|) = \begin{cases} 0 & \text{if } \|\mathbf{e}\| < \varepsilon, \\ \|\mathbf{e}\| & \text{otherwise,}\end{cases}$$

any user-defined tracking precision $\varepsilon > 0$ can ultimately be met[4]. This can be seen by noticing that $\kappa(t)$ and $\varphi(t)$ grow for all t due to the integral when $\|\mathbf{e}\| \geq \varepsilon$. As a consequence, the maximum value of $\|\mathbf{r}\|$ such that $\dot{V}(\mathbf{r})$ is surely negative decreases. It does so because $h_2(\mathbf{r})$ in (31) is non-positive for

[4]Please note that the use of $f(\|\mathbf{e}\|) = \alpha$ when $\|\mathbf{e}\| \geq \varepsilon$ with a positive constant α can also be considered.

$\|\mathbf{r}\| \geq \max\left(\frac{\beta_d}{\varphi(t)\,\delta}, \frac{1}{\kappa(t)}\right)$. Then, there will be a large enough $t_2 > t_1$ such that $\max\left(\frac{\beta_d}{\varphi(t_2)\,\delta}, \frac{1}{\kappa(t_2)}\right)$ is small enough, since

$$\|\mathbf{r}\| \leq \max\left(\frac{\beta_d}{\varphi(t_2)\,\delta}, \frac{1}{\kappa(t_2)}\right)\sqrt{\frac{\lambda_M}{\lambda_m}}$$
$$< \max\left(\frac{\beta_d}{\varphi(t_1)\,\delta}, \frac{1}{\kappa(t_1)}\right)\sqrt{\frac{\lambda_M}{\lambda_m}}.$$

This allows that, for $t \geq t_2$, the trajectories $\mathbf{r}$ ultimately stay within a ball small enough such that $\|\mathbf{e}\| < \varepsilon$, for any selection of the gains $\mathbf{K}_r$. The block diagram of the IA-PB controller is presented in Figure 2.

Remark 2: By considering Remark 1, this time for $\mathbf{w}_{PB}(\mathbf{q}, \dot{\mathbf{q}}, \dot{\mathbf{q}}_a, \ddot{\mathbf{q}}_a, \boldsymbol{\Delta}_0, \boldsymbol{\Delta}, \mathbf{d})$ and $\boldsymbol{\rho}\left([\boldsymbol{\Phi}_{PB}]\right)$, continuity of (29) and (30) also follows.

Remark 3: The perturbation functions in (7) and (23) are Lipschitz continuous with respect to the uncertain parameters as follows from assumption 4 in Subsection II-B. Furthermore, from assumption 1 in Subsection II-B, we have that all uncertain parameters are bounded. As a consequence, evaluating the effect of uncertain parameters in (7) and (23) using interval arithmetic results in bounded ranges [40, Chapter 6].

Remark 4: The use of interval arithmetic in our schemes does not introduce a wrapping effect (see e.g., [44]) since each evaluation of (8) and (25) does not rely on results from previous evaluations. Furthermore, over-approximations resulting from interval arithmetic do not destabilize the system since our schemes ensure specified error bounds for any bounded uncertainty. The limited impact of over-approximations is further discussed in Subsection III-D and shown by experiments in Subsection IV-D.

C. Identification of bounds for inertial parameters

In this subsection we propose an approach for tight identification of the bounds of the inertial parameters. Manually determined bounds of the uncertain parameters $[\boldsymbol{\Delta}], [\mathbf{d}]$ may lead to an overly conservative estimation of the intervals $[\boldsymbol{\Phi}_{ID}]$ or $[\boldsymbol{\Phi}_{PB}]$ due to the dependency problem of interval arithmetic, which then leads to unnecessarily conservative robustifying control actions. For finding tight $[\boldsymbol{\Delta}], [\mathbf{d}]$, we consider model conformance [45], which establishes a formal link between an abstraction and the real behaviour of a system. We introduce the inverse dynamics model

$$\mathbf{w}^*(\mathbf{q}, \dot{\mathbf{q}}, \dot{\mathbf{q}}^*, \ddot{\mathbf{q}}^*, \boldsymbol{\Delta}, \mathbf{d}) := \boldsymbol{\tau}^* = \mathbf{M}(\mathbf{q}, \Delta)\ddot{\mathbf{q}}^* + \mathbf{C}(\mathbf{q}, \dot{\mathbf{q}}, \Delta)\dot{\mathbf{q}}^* + \mathbf{f}(\dot{\mathbf{q}}, \Delta) + \mathbf{g}(\mathbf{q}, \Delta) - \mathbf{d},$$

where $\boldsymbol{\tau}^*$ is the output and $\mathbf{q}, \dot{\mathbf{q}}, \dot{\mathbf{q}}^*, \ddot{\mathbf{q}}^*$ are the inputs. The above model is an abstraction of the real mechanical system and is subsequently used to compute the bounds $[\boldsymbol{\Phi}_{ID}]$ and $[\boldsymbol{\Phi}_{PB}]$, which can then be rewritten as

$$[\boldsymbol{\Phi}_{ID}] = \mathbf{w}^*(\mathbf{q}, \dot{\mathbf{q}}, \dot{\mathbf{q}}, \mathbf{y}, [\boldsymbol{\Delta}], [\mathbf{d}]) - \mathbf{w}^*(\mathbf{q}, \dot{\mathbf{q}}, \dot{\mathbf{q}}, \mathbf{y}, \boldsymbol{\Delta}_0, \mathbf{0}) \quad (34)$$
$$[\boldsymbol{\Phi}_{PB}] = \mathbf{w}^*(\mathbf{q}, \dot{\mathbf{q}}, \dot{\mathbf{q}}_a, \ddot{\mathbf{q}}_a, [\boldsymbol{\Delta}], [\mathbf{d}]) - \mathbf{w}^*(\mathbf{q}, \dot{\mathbf{q}}, \dot{\mathbf{q}}_a, \ddot{\mathbf{q}}_a, \boldsymbol{\Delta}_0, \mathbf{0}). \quad (35)$$

To ensure robustness of the real mechanical system, the reachable sets in (34) and (35) computed using the abstract model must at least overapproximate the reachable set of the real system that is affected by uncertainties. To establish this formal link, *reachset conformance testing* [46] is suitable: since the real reachable set is not directly measurable, we instead measure the outputs generated by the real system and check whether the bounds of our abstract model include all test results (see Figure 3).

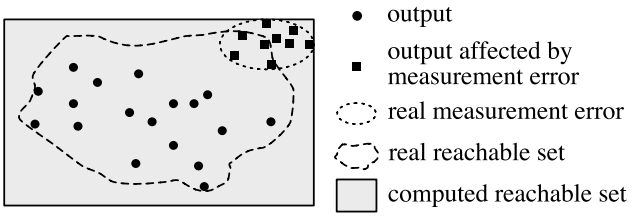

Fig. 3. The above picture shows that the computed reachable set overapproximates the real one, as well as included measurment errors. Thus, the underlying model is reachset conformant.

We define a model as reachset conformant, if for each test case $i = 1..L$ the measured output $\boldsymbol{\tau}^*_{m,i}$ is included in the reachable set $[\boldsymbol{\tau}^*] = \mathbf{w}^*(.)$ determined by the inputs $\mathbf{q}_i, \dot{\mathbf{q}}_i, \dot{\mathbf{q}}^*_i, \ddot{\mathbf{q}}^*_i$ and the parameters $[\boldsymbol{\Delta}], [\mathbf{d}]$:

$$\forall i \in [1, L]: \quad \boldsymbol{\tau}^*_{m,i} \in \mathbf{w}^*(\mathbf{q}_i, \dot{\mathbf{q}}_i, \dot{\mathbf{q}}^*_i, \ddot{\mathbf{q}}^*_i, [\boldsymbol{\Delta}], [\mathbf{d}]). \quad (36)$$

The input-output pairs can be obtained by measuring the actuation commands $\boldsymbol{\tau}_J$, the position $\mathbf{q}$, velocity $\dot{\mathbf{q}}$, and acceleration $\ddot{\mathbf{q}}$. Thus, we set $\boldsymbol{\tau}^*_m := \boldsymbol{\tau}_J$, $\dot{\mathbf{q}}^* := \dot{\mathbf{q}}$, and $\ddot{\mathbf{q}}^* := \ddot{\mathbf{q}}$. Since (36) is expressed as a constraint, we determine the best $[\boldsymbol{\Delta}], [\mathbf{d}]$ by formulating a constrained optimization problem minimizing the size of the set $[\boldsymbol{\tau}^*]$:

$$\min_{[\boldsymbol{\Delta}], [\mathbf{d}]} \sum_{i=1}^{L} (\overline{\boldsymbol{\tau}}^*_i - \underline{\boldsymbol{\tau}}^*_i)^2$$
$$\text{s.t.} \quad \forall i : \boldsymbol{\tau}_{J,i} \in [\boldsymbol{\tau}^*_i],$$

where $[\boldsymbol{\tau}^*_i] = [\overline{\boldsymbol{\tau}}^*_i, \underline{\boldsymbol{\tau}}^*_i] = \mathbf{w}^*(\mathbf{q}_i, \dot{\mathbf{q}}_i, \dot{\mathbf{q}}_i, \ddot{\mathbf{q}}_i, [\boldsymbol{\Delta}], [\mathbf{d}])$. This procedure requires a sufficient number L of test cases, to sufficiently cover the measurement error of the inputs and outputs, as shown in Figure 3 for a simple example. A sufficient number of tests L has been conducted if the identification results are the same for all the additional tests that can be afforded. If desired, an additional safety factor can be considered, which does not significantly affect the performance as shown in Subsection IV-D. Note that the above optimization problem is an inverse dynamics version of the one proposed in [47] for the forward dynamics.

Remark 5: This technique is suitable for mechanical systems which have a nonlinear model structure. However, if the model structure is linear, then the constraint in (36) is also linear. If we then consider the cost as the 1-norm instead of the 2-norm, the optimization problem can be globally solved through linear programming [48].

D. Discussion

It is important to consider that other existing controllers with discontinuous or adaptive control laws can guarantee asymptotic tracking in principle (see e.g., [18], [49]). However,

this often comes at the price of introducing chattering and loss of robustness. On the one hand, when considering classical discontinuous robust control schemes, chattering can be avoided by including a smoothing modification at the cost of a reduced tracking performance (see e.g., [9, Section 8.5.3]). On the other hand, adaptive control schemes typically require linearly parametrized perturbation functions, as well as changes to the control laws to avoid loss of robustness when fast adaptation is desired [50]. In the above mentioned cases, one faces the loss of asymptotic tracking capabilities and non-trivial tuning of the parameters involved in the modifications. Moreover, existing classical robust controllers can be very conservative due to the need for obtaining bounds of nonlinear state-dependent perturbations for the entire state space as we further describe in Section IV.

In contrast to previous approaches, our method does not require time-consuming procedures for estimating bounds of perturbations from model uncertainties, which are even non-formal in previous approaches. As opposed to adaptive control, where the control law is adapted with respect to online-extracted knowledge of plant parameters, the integral action of $\kappa(t)$ and $\varphi(t)$ results in an automatic robust control gain increase. Our proposed schemes are often simpler to implement in practice with respect to adaptive counterparts as they do not require one to linearly parametrize the perturbation with regressors.

Particularly promising applications of this approach are those requiring deployment of guaranteed robust controllers automatically, with little to no intervention of control-designers. This is the case, e.g., of modular reconfigurable robot manipulators whose deployment is desired to be effortless [51] after arbitrary assembly, to preserve the benefits from swift reconfigurability. To this end, our proposed control approach can be combined with the framework in [52] for achieving the automatic deployment of robust controllers after arbitrary assembly of modular reconfigurable robot arms.

The benefits introduced by the interval-arithmetic-based robust controllers come at the price of an increased computational complexity with respect to conventional schemes. For both the inverse-dynamics and the passivity-based version, a simple way to implement the controller is to use a software with symbolic manipulation capabilities and obtain the perturbation functions $\mathbf{w}_{ID}$ or $\mathbf{w}_{PB}$ analytically. Then, software packages which support interval arithmetic computations can be used for evaluating online these functions with the appropriate interval arguments, such as [41], [42].

When considering serial robot manipulators, an algorithm for efficient computation of the perturbation functions can be found in [53]. That work introduces the idea of using set-based operations in recursive Newton-Euler algorithms [54], [55]. The proposed approach allows the computation of formally guaranteed over-approximative sets of perturbing torques/forces, arising from imperfect knowledge of dynamic model parameters. It allows one to perform the computations required for obtaining $\boldsymbol{\rho}([\boldsymbol{\Phi}_{ID}])$ or $\boldsymbol{\rho}([\boldsymbol{\Phi}_{PB}])$ efficiently, with a computational complexity that grows linearly with the number of degrees of freedom. This allows us to carry out these computations numerically online for robots with many degrees of freedom as well, without the need for software with symbolic variable manipulation capabilities. In this work we employ the approach in [53] for efficiently implementing all the interval-arithmetic-based robust controllers of the experiments on a six-degrees-of-freedom robot manipulator in Section IV.

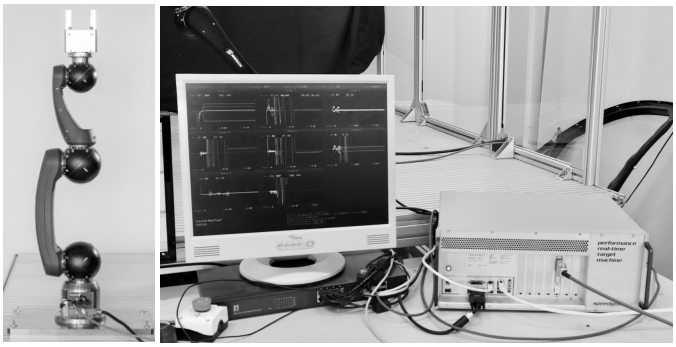

Fig. 4. Testbed used for the experiments.

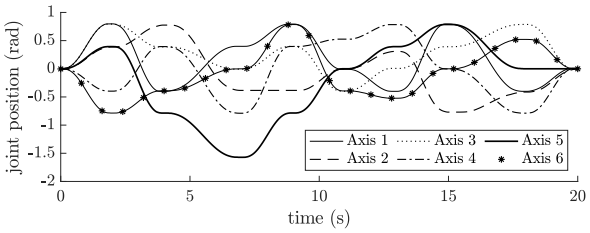

Fig. 5. Test trajectory used for the experiments.

The conservatism that is introduced in practice with our approach has shown to be limited even when dealing with systems with highly nonlinear coupled dynamics, such as robot manipulators [38], [53]. Since we have no wrapping effect as described in Remark 4, we do not require more elaborated approaches for obtaining less conservative over-approximations of the perturbations, such as zonotopes, which are computationally more expensive and harder to implement.

IV. Experiments

Our experiments are carried out on a Schunk LWA-4P robot, controlled by a Speedgoat Performance Target Machine with sampling time of 4ms (see Figure 4). We recall the essence of other control schemes for benchmarking in Subsection IV-A, and we experimentally evaluate the controllers in Subsections IV-B, IV-C, and IV-D. The interval arithmetic has been implemented as described in Subsection III-D and the test trajectory used for these experiments can be seen in Figure 5.

The bounds for the inertial parameters we use in the experiments have been identified with the approach described in Subsection III-C. With this approach a sufficient amount of testing data is needed until $[\boldsymbol{\Delta}], [\mathbf{d}]$ stop increasing. In this paper, we collect test data by means of multiple executions of the relevant trajectory in Figure 5 with an arbitrary controller and manually stop the testing with $L = 22254$. An alternative way is to choose test cases that bring the most probable improvements using Bayesian optimization. The resulting Gaussian process model is then also used as a test

end criterion by defining a lower threshold for the probability of a failing test case [56]. For our robot system, we use the Interval Arithmetic Based Newton-Euler Algorithm (IANEA) [53] including the friction model of [57] to compute $\mathbf{w}^*(.)$. The robot consists of motor current sensors for measuring joint torques, and encoders for measuring the positions. The velocity is obtained online through a moving-average filter [32], and the acceleration (only needed for offline identification) is obtained through zero-phase-shift digital filtering. We use the local constraint solver `fmincon` in MATLAB to find the optimal supremum and infimum of the intervals $[\boldsymbol{\Delta}], [\mathbf{d}]$. We limit the search-space by providing manually-determined bounds as upper and lower limits, and also use these bounds as an initial guess for the local optimization. In Figure 6 we show the effectiveness of this identification technique by providing tight torque estimations and comparing them to torques measurements.

A. Essentials of benchmark control schemes

In this subsection we briefly recall the essence of the schemes used for benchmarking. Three approaches are considered, as they are representative of benefits and limitations of existing schemes: *i)* a classical robust control approach that can provide asymptotic tracking in principle, but whose application in a real system requires estimation of bounds of state-dependent uncertain model terms and smoothing; *ii)* a robust control approach that can provide robust performance with a continuous controller, but that requires estimation of bounds similar to (*i*); *iii)* a recent adaptive-robust control scheme that can provide GUUB and does not require bounds or prior knowledge of uncertain parameters, but that has a discontinuous control law.

1) Classical robust control: A classical approach that can be used for robust control of fully-actuated mechanical systems is the enhancement of a nominal inverse-dynamics control scheme by means of a robust control term obtained from Lyapunv's second method [9] and the following assumptions[5]:

$$\begin{gathered}
0 < B_m \leq \|\mathbf{M}(\mathbf{q},\boldsymbol{\Delta})^{-1}\| \leq B_M < \infty \quad \forall \mathbf{q},\, \boldsymbol{\Delta} \in [\boldsymbol{\Delta}], \\
\|\mathbf{I} - \mathbf{M}(\mathbf{q},\boldsymbol{\Delta})^{-1}\mathbf{M}_0(\mathbf{q})\| \leq \alpha_{cr} \leq 1 \quad \forall \mathbf{q},\, \boldsymbol{\Delta} \in [\boldsymbol{\Delta}], \\
\|\mathbf{n}_0(\mathbf{q},\dot{\mathbf{q}}) - \mathbf{n}(\mathbf{q},\dot{\mathbf{q}},\boldsymbol{\Delta})\| < \eta_{cr} \quad \forall \mathbf{q},\, \dot{\mathbf{q}},\, \boldsymbol{\Delta} \in [\boldsymbol{\Delta}], \\
\max(\|\ddot{\mathbf{q}}_d\|) < Q_M < \infty \quad \forall \ddot{\mathbf{q}}_d,
\end{gathered}$$

for some positive constants B_m, B_M, α_{cr}, η_{cr}, Q_M. With this approach the robust control law can be implemented as

$$\mathbf{u} = \mathbf{M}_0(\mathbf{q})\left(\ddot{\mathbf{q}}_d + \mathbf{K}_D\dot{\mathbf{e}} + \mathbf{K}_P\mathbf{e} + \boldsymbol{\nu}_{cr}\right) + \mathbf{n}_0(\mathbf{q},\dot{\mathbf{q}}),$$

$$\boldsymbol{\nu}_{cr} = \begin{cases} \frac{\rho_{cr}(\boldsymbol{\xi})}{\|\mathbf{z}\|}\mathbf{z}, & \|\mathbf{z}\| \geq \delta, \\ \frac{\rho_{cr}(\boldsymbol{\xi})}{\delta}\mathbf{z}, & \|\mathbf{z}\| < \delta, \end{cases}$$

with $\delta > 0$, $\mathbf{z} = \mathbf{B}^T\mathbf{P}\boldsymbol{\xi}$ and

$$\rho_{cr}(\boldsymbol{\xi}) \geq \frac{1}{1-\alpha_{cr}}\left(\alpha_{cr}Q_M + \alpha_{cr}\|(\mathbf{K}_P, \mathbf{K}_D)\|\|\boldsymbol{\xi}\| + B_M\eta_{cr} + \beta_d\right).$$

[5]In this case it is considered that $\mathbf{M}_0 = 2/(B_M + B_m)\mathbf{I}$ to get $\alpha_{cr} \leq 1$ as suggested in [9].

The above terms $\boldsymbol{\xi}$, $\mathbf{P}$, and $\mathbf{B}$ are the same as those in (11), (12) and (13).

With this scheme, GUUB is ensured and the error bounds depend on δ, i.e., the larger δ is, the larger the resulting bounds on the tracking error norm are [9]. When an increase of the tracking performance is desired, one can reduce δ. However, even though global asymptotic stability can theoretically be shown for $\delta = 0$, the chattering phenomenon may be problematic for real-world deployment, especially since a discontinuous control law is approached by reducing δ. Additionally, this robust control approach can be highly conservative due to the need for obtaining the considered bounds for the entire, practically-reachable state space.

2) r-α tracking control: The r-α tracker was introduced in [14]. After a study of the uncertain model components for obtaining specific uncertainty bounds, the control law can be implemented without requiring model-based computations online. Interestingly, such a control scheme guarantees in principle the tracking of a desired trajectory with a prescribed rate of convergence α within a user-defined bound r. Since the bound r can be selected by the user a priori, the approach qualifies for providing robust performance control. As described in [14], the controller design process starts from the computation of the uncertainty bounds β_i for $i \in \{0,\ldots,3\}$, for all $\mathbf{q}$, $\dot{\mathbf{q}}$, $\mathbf{d} \in [\mathbf{d}]$ and $\boldsymbol{\Delta} \in [\boldsymbol{\Delta}]$ such that

$$\begin{gathered}
\lambda_{min}\left(\mathbf{M}(\mathbf{q},\boldsymbol{\Delta})\right) \geq \beta_0 \geq 0, \;\; \lambda_{max}\left(\mathbf{M}(\mathbf{q},\boldsymbol{\Delta})\right) \leq \beta_1, \\
\|\mathbf{C}(\mathbf{q},\dot{\mathbf{q}},\boldsymbol{\Delta})\| \leq \beta_2\|\dot{\mathbf{q}}\|, \;\; \|\mathbf{g}(\mathbf{q},\boldsymbol{\Delta}) - \mathbf{d}\| \leq \beta_3.
\end{gathered}$$

Once these bounds are computed, an additional tuning parameter δ_{zc} and two symmetric positive definite matrices ($\boldsymbol{\Lambda}_{zc}$, $\mathbf{Q}_{zc}$) are selected such that

$$\begin{gathered}
\lambda_{min}(\boldsymbol{\Lambda}_{zc}) \geq \alpha, \; \lambda_{min}(\mathbf{Q}_{zc}) \geq \alpha\beta_1, \\
\delta_{zc} \leq (\alpha r)^2\lambda_{min}(\mathbf{Q}_{zc})\,\beta_0/\beta_1.
\end{gathered}$$

The r-α tracking controller is implemented as follows [14]:

$$\begin{gathered}
\mathbf{u} = \mathbf{Q}_{zc}\mathbf{r} + \left(\|\rho_{zc}\mathbf{r}\| + \delta_{zc}\right)^{-1}\rho_{zc}^2\mathbf{r}, \\
\rho_{zc} = \beta_1\|\ddot{\mathbf{q}}_a\| + \beta_2\|\dot{\mathbf{q}}_a\|\|\dot{\mathbf{q}}\| + \beta_3.
\end{gathered}$$

In the above equation, the term $\dot{\mathbf{q}}_a$ is the same as in (20) and $\mathbf{r} = \dot{\mathbf{e}} + \boldsymbol{\Lambda}_{zc}\mathbf{e}$. Similar to the classical robust control case, non-formal sampling procedures for estimating the required bounds are typically necessary.

3) Adaptive sliding-mode control: Among the most recent schemes for robust control, [28] proposes an adaptive sliding-mode control scheme that, interestingly, does not need the a priori knowledge of bounds of nonlinear state-dependent model terms. This controller can provide GUUB and is implemented as follows [28]:

$$\mathbf{u}_{asm} = \boldsymbol{\Lambda}_{asm}\mathbf{r} + \rho(t)\mathrm{sgn}(\mathbf{r}) \tag{37}$$

where $\mathbf{r} = \dot{\mathbf{e}} + \mathbf{Q}_{asm}\mathbf{e}$, with $\boldsymbol{\Lambda}_{asm}$ and $\mathbf{Q}_{asm}$ being positive definite matrices of proper dimensions. The term $\rho(t)$ includes the adaptive contribution and is computed as

$$\rho(t) = \hat{K}_0(t) + \hat{K}_1(t)\|\boldsymbol{\xi}(t)\| + \hat{K}_2(t)\|\boldsymbol{\xi}(t)\|^2,$$

where

$$\dot{\hat{K}}_i(t) = \|\mathbf{r}\|\|\boldsymbol{\xi}(t)\|^i - \alpha_i\|\boldsymbol{\xi}(t)\|,$$

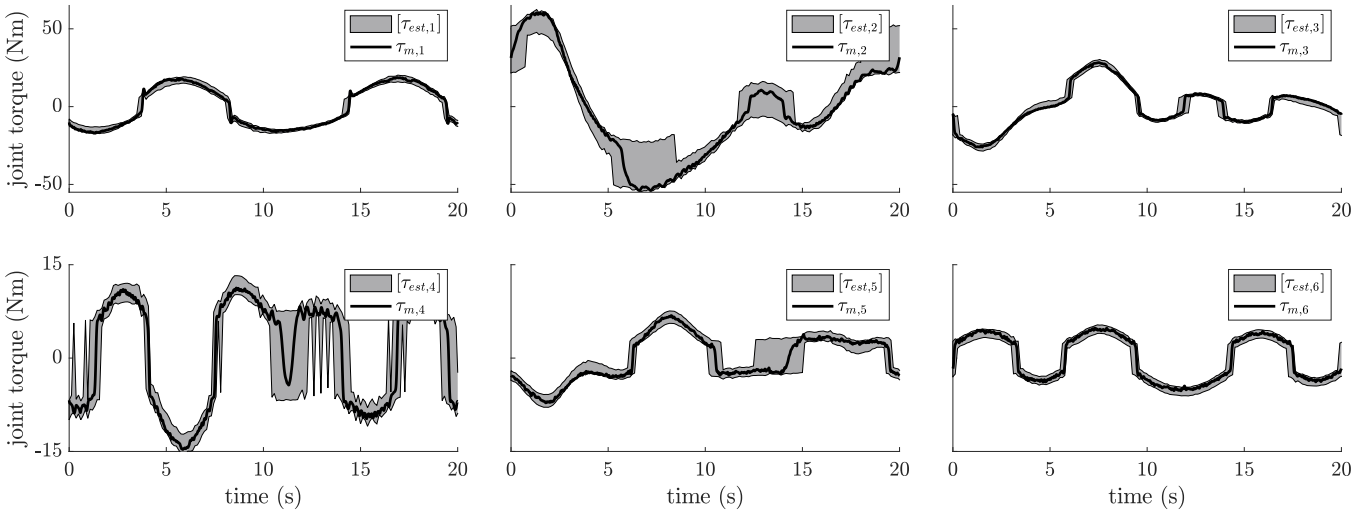

Fig. 6. Identification results showing that the identified parameter sets $[\mathbf{\Delta}], [\mathbf{d}]$ lead to a tight overapproximation $[\boldsymbol{\tau}^*]$ of the measured motor torque $\boldsymbol{\tau}_m$.

and $\dot{\hat{K}}_i(0) > 0$, $\alpha_i > 0$ and $i \in \{0,\ldots,2\}$.

B. Experimental performace evaluation with IA-ID

In this subsection we present the experimental results of our proposed IA-ID controller by demonstrating ultimate boundedness of the tracking error and by comparing its performance with respect to the classical robust control scheme. Please note that for the comparisons in this and the following subsection, we describe the considerations we made for maintaining a fair selection of the tuning parameters. In particular, this selection has been performed manually by exploiting control law similarities form one scheme another when possible, and by selecting gains leading to comparable measurement noise amplification on the control commands while trying to obtain the best possible performance.

To deploy the classical robust control scheme, we obtain the needed state-dependent bounds using a sampling procedure with 10^5 samples within the identified sets of inertial parameters. Then we set the following tuning parameters:

$$\mathbf{K}_P = 225\mathbf{I},\ \mathbf{K}_D = 19.5\mathbf{I},\ \mathbf{Q} = \begin{bmatrix} 10\mathbf{I} & 0 \\ 0 & \mathbf{I} \end{bmatrix}. \tag{38}$$

To obtain the best performance, we determine the lowest δ that does not introduce excessive chattering of the control commands, resulting in $\delta = 0.4$. This selection is non-trivial since severe chattering can be faced while tuning δ because ρ_{cr} results in a highly conservative term. For a fair selection of the gains of our proposed IA-ID controller, we can exploit the control scheme similarity. In fact, we select $\mathbf{K}_P$, $\mathbf{K}_D$, $\mathbf{Q}$ equally as in (38). To obtain the best performance, we increase κ_P such that the error norm is minimized while maintaining similar measurement noise amplification compared to the classical robust control scheme. Following this approach, we set $\kappa_P = 3$. Tuning the parameter κ_P of the robustifying part is intuitive since its increase directly makes the tracking error decrease. On the other hand, the increase of this parameter increases the effect of the amplification of the measurement noise on the current commands. The tuning procedure aims at finding a trade-off between tracking precision and noise amplification. Since we fix $\mathbf{K}_P$, $\mathbf{K}_D$, $\mathbf{Q}$ to be the same for the two schemes, we are able to assess the impact of the robustifying terms on the performance, thus making a direct comparison between classical robust control and IA-ID control.

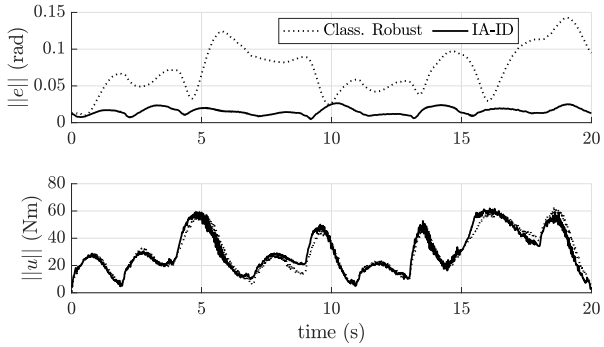

Fig. 7. Performance comparison between the classical robust control scheme and interval-arithmetic inverse-dynamics control.

The results of this experiment are shown in Figure 7: we can observe that IA-ID reaches an overall lower error. Additionally, the IA-ID approach remarkably removes the need for obtaining bounds of highly nonlinear state-dependant model terms, contrary to the classical robust controller. Furthermore, thanks to the approach adopted here for online computing the worst-case perturbation using IANEA, as we proposed in [53], IA-ID was significantly less conservative and drastically reduced chattering effects when tuning it.

C. Experimental performace evaluation with IA-PB

In this subsection we present the performance of our proposed IA-PB control scheme with respect to the benchmark schemes considered. To deploy the r-α tracker, we obtain the needed bounds on state-dependent model terms by taking 10^5

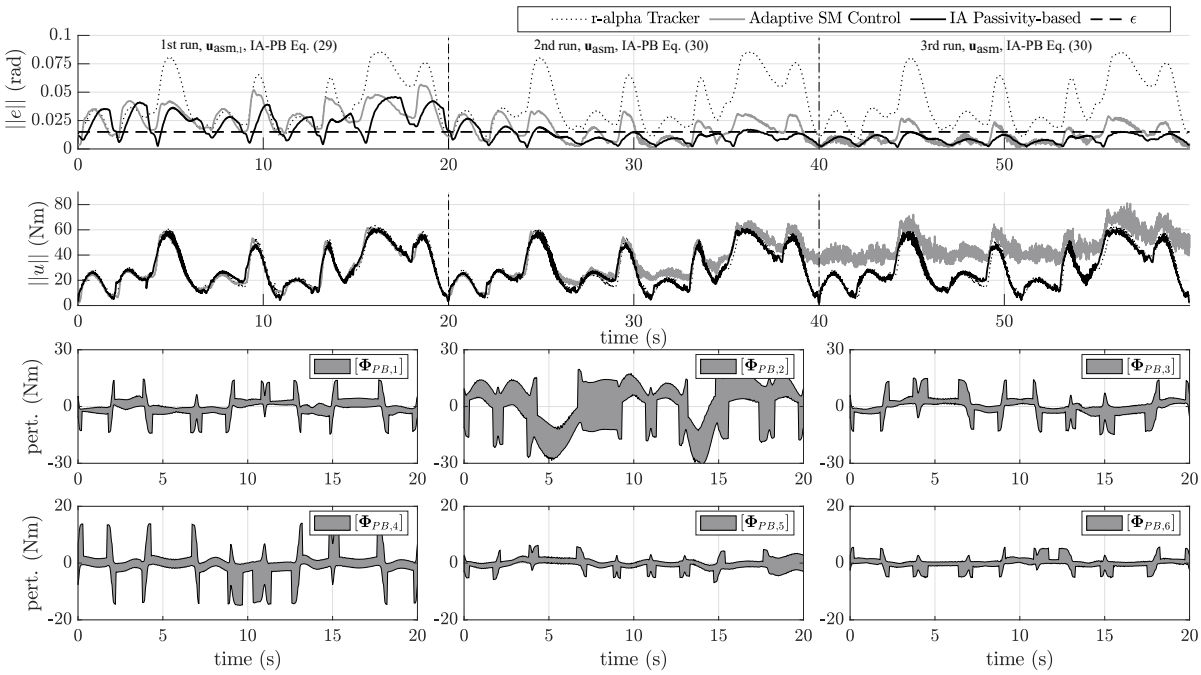

Fig. 8. Comparison of robust performance: $\varepsilon = 0.015\,rad$, and we run the trajectory three times. In the first run, the IA-PB controller uses (29), and the adaptive sliding-mode controller uses $\mathbf{u}_{\text{asm},1}$. In subsequent runs, the IA-PB controller uses (30) and the adaptive sliding-mode controller uses (37).

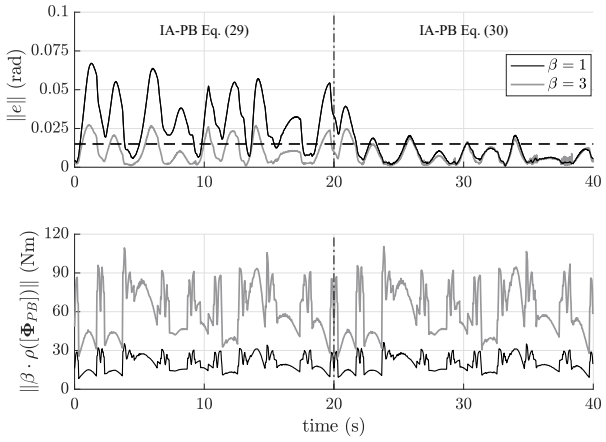

Fig. 9. Experimental results showing the effect of interval arithmetic over-approximations on the tracking performance.

samples from the identified sets of inertial parameters $[\mathbf{\Delta}]$. This controller has shown to be highly conservative, making it difficult to deploy in practice due to severe chattering. In this experiment we use $\mathbf{Q}_{zc} = \alpha\beta_1\,\mathbf{I}$ and $\mathbf{\Lambda}_{zc} = \alpha\,\mathbf{I}$. Then, we set the parameters $r = 5$, $\alpha = 10$ that are large enough to avoid chattering while trying to maintain the lowest possible tracking error in this case.

We deploy the considered adaptive sliding-mode controller with $\mathbf{\Lambda}_{asm} = \text{diag}(25,40,25,25,25,25)$, $\mathbf{Q}_{asm} = \text{diag}(25,40,25,25,25,25)$, $\alpha_1 = 0.07$, and $\alpha_{2,3} = 0.3$. For comparison, we introduce a case in which $\mathbf{u}_{asm,1} = \mathbf{\Lambda}_{asm}\mathbf{r}$, thus without using any adaptive-robust term, and the complete scheme as in (37). The parameters $\mathbf{\Lambda}_{asm}$ and $\mathbf{Q}_{asm}$ have been selected such that the tracking performance using $\mathbf{u}_{\text{asm},1}$ is similar to the tracking performance of the IA-PB control variant that provides GUUB. The adaptive parameters $\alpha_{1,2,3}$ have been chosen such that a maximum error decrease is achieved with a similar measurement noise amplification compared to IA-PB. We experienced difficulties in the implementation due to the high sensitivity to control input chattering when selecting these parameters.

The control parameters of our proposed IA-PB scheme have been selected as

$$K_r = 15,\ \kappa_P = 1,\ \phi_P = 1,\ \kappa_I = 2,\ \phi_I = 500.$$

These parameters have been chosen such that a maximum error reduction is achieved to maintain a comparable measurement noise amplification on the control commands, as provided by the other considered benchmarks.

The results of this experiment are presented in Figure 8 showing the performance of the r-α tracker, the considered adaptive sliding-mode scheme, and our proposed IA-PB control. For these tests, we assume a desired performance with $\varepsilon = 0.015\,rad$ and we let the desired test trajectory run for three consecutive times. In the first run, the robust-adaptive term is disabled to validate that we fairly tuned the controller, that can be observed from the similar tracking performance we allowed. At the start of the second run of the trajectory (at $t = 20s$) we activate the complete adaptive sliding-mode scheme resulting in a slight increase of performance over time and we observe chattering effects. Chattering can be observed more clearly in the third run with the considered adaptive sliding-mode controller, for which it was not possible

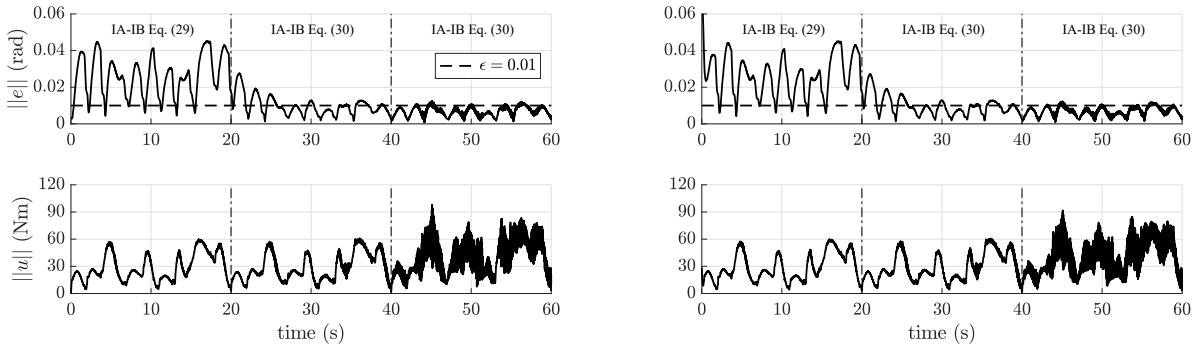

Fig. 10. Further experimental results of the IA-PB controller with $\varepsilon = 0.01\,rad$. Left shows performance for $\|\mathbf{e}(0)\| = 0\,rad$, right shows performance for $\|\mathbf{e}(0)\| = 0.1225\,rad$.

to further reduce the tracking error in this case. Such undesired behaviour is also reflected by the norm of torque commands, which shows an undesired slight increase over time with no further noticeable improvement of the tracking error. On the other hand, also at $t = 20s$, we activate the complete IA-PB control scheme for achieving the desired robust performance, causing a quick and smooth error decrease. With IA-PB, after 25 seconds, the error only occasionally increases over ε and is gently driven down to the limit by the integral action to provide robust performance. Figure 8 also displays the online-computed continuous bounds using interval arithmetic for each axis, adopted by the robustifying term of IA-PB control.

Overall, the IA-PB controller delivers the best performance in practice with respect to the other controllers considered. In particular, with the considered setting, the r-α tracker and the chosen adaptive sliding-mode controller are incapable of reaching $\varepsilon = 0.015\,rad$ without excessive chattering, contrary to IA-PB. The considered adaptive sliding-mode controller, although having the remarkable merit of not requiring a priori bounds of model terms, has a discontinuous control law and finding suitable adaptive action parameters is challenging due to high chattering sensitivity as we experienced in practice.

D. Practical considerations

Although over-approximations are reduced through using our model identification approach, we demonstrate their potential impact on stability by experimental results in Figure 9. This experiment was performed with the same setting as in Figure 8, with and without enlargement of the intervals by a factor β. The results show that over-approximations do not introduce a destabilizing effect.

Our proposed IA-PB controller provides robust performance thanks to the integral actions in $\kappa(t)$ and $\phi(t)$. However, although arbitrary performance can be reached in principle, physical limits of the actuators can be encountered in practice. For illustrating and discussing this better, we present additional experimental results of our proposed IA-PB controller in Figure 10. Considering the same control parameters of the experiment in Figure 8, we set the desired performance to a more strict value by reducing ε to $0.01\,rad$. The test trajectory is run three times in this experiment. The first column of Figure 10 shows the robust performance at zero initial condition $\|\mathbf{e}(0)\| = 0\,rad$. Measurement noise amplification on the control commands can be seen when the trajectory is run for the second time (for $t > 20s$). The second column of Figure 10 shows that the robust controller is smoothly converging also when facing mismatched initial conditions (in this case with $\|\mathbf{e}(0)\| = 0.1225\,rad$). In this second case the integral actions are only activated at $t = 1s$, to avoid excessive conservativity that can be otherwise reached. In fact, the increase in performance also results in an amplification of the measurement noise on the control command. As one can reasonably expect, these effects are those that impose physical limits on the achievable tracking performance in practice. This problem becomes worse, as the integral actions surge when setting large initial errors. For practical implementation, we recommend to stop the integral action during the first transient from large mismatches in the initial conditions and when the amplification of the noise becomes unacceptable for the actuators at hand. When postponing the start after the first transient or stopping these integrals before the desired performance is met, GUUB is still maintained as shown in (33). The realized mismatch for the initial conditions is representative for showing the typical transient performance we experienced in practice.

V. Conclusion

A novel approach for robust control of fully-actuated mechanical systems is introduced, achieving both ultimate boundedness of the tracking error and robust performance, and avoiding the need for manual estimation of bounds of nonlinear state-dependent perturbation functions. Our proposed method does not require the linearity property of the mechanical system and can be applied even when the dynamics are highly nonlinear and coupled. Further, it results in continuous control laws, which is particularly interesting for mechanical systems to avoid vibrations or damaging actuators.

Experimental results using a six degrees-of-freedom robot manipulator show the real-world applicability and the effectiveness of the proposed approach with respect to relevant existing methods. A particularly interesting practical aspect is that our approach can be quickly deployed since it is fully automatic. This is especially useful for robust control of modular and reconfigurable systems.

ACKNOWLEDGMENT

The research leading to these results has received funding from the European Unions Horizon 2020 research and innovation program under grant agreement No 101016007 (project CONCERT).

REFERENCES

[1] R. Freeman and P. V. Kokotovic, *Robust nonlinear control design: state-space and Lyapunov techniques*. Springer Science & Business Media, 2008.

[2] S. Mitra, T. Wongpiromsarn, and R. M. Murray, "Verifying cyber-physical interactions in safety-critical systems," *IEEE Security Privacy*, vol. 11, no. 4, pp. 28–37, July 2013.

[3] A. Pereira and M. Althoff, "Safety control of robots under computed torque control using reachable sets," in *Proc. IEEE Int. Conf. on Robotics and Automation*, 2015, pp. 331–338.

[4] D. A. Bristow and A. G. Alleyne, "A high precision motion control system with application to microscale robotic deposition," *IEEE Trans. Control Syst. Technol.*, vol. 14, no. 6, pp. 1008–1020, 2006.

[5] J. Qiao, H. Wu, and X. Yu, "High-precision attitude tracking control of space manipulator system under multiple disturbances," *IEEE Trans. Syst., Man, Cybern. Syst.*, vol. 51, no. 7, pp. 4274–4284, 2021.

[6] R. Ortega, J. A. L. Perez, P. J. Nicklasson, and H. J. Sira-Ramirez, *Passivity-based control of Euler-Lagrange systems: mechanical, electrical and electromechanical applications*. Springer Science & Business Media, 2013.

[7] C. C. de Wit, B. Siciliano, and G. Bastin, Eds., *Theory of Robot Control*. Springer-Verlag London, 1996.

[8] M. W. Spong, S. Hutchinson, and M. Vidyasagar, *Robot Modeling and Control*. Wiley, 2006.

[9] B. Siciliano, L. Sciavicco, L. Villani, and G. Oriolo, *Robotics: Modelling, Planning and Control*. Springer, 2009.

[10] B. Brogliato, R. Lozano, B. Maschke, and O. Egeland, *Dissipative systems analysis and control: Theory and Applications*. Springer International Publishing, 2020.

[11] C. Abdallah, D. Dawson, P. Dorato, and M. Jamshidi, "Survey of robust control for rigid robots," *IEEE Control Systems*, vol. 11, no. 2, pp. 24–30, Feb. 1991.

[12] M. Spong, "On the robust control of robot manipulators," *IEEE Trans. on Automatic Control*, vol. 37, no. 11, pp. 1782–1786, 1992.

[13] G.-J. Liu and A. Goldenberg, "On robust saturation control of robot manipulators," in *Proc. of the 32nd IEEE Conference on Decision and Control*, 1993, pp. 2115–2120 vol.3.

[14] S. Zenieh and M. Corless, "Simple robust r - α tracking controllers for uncertain fully-actuated mechanical systems," *ASME J. Dyn. Sys., Meas., Control*, vol. 119, no. 4, pp. 821–825, 1997.

[15] F. Lin and R. Brandt, "An optimal control approach to robust control of robot manipulators," *IEEE Trans. on Robotics and Automation*, vol. 14, no. 1, pp. 69–77, 1998.

[16] J. Park and W. K. Chung, "Analytic nonlinear H_∞ inverse-optimal control for Euler-Lagrange system," *IEEE Trans. Robot. and Autom.*, vol. 16, no. 6, pp. 847–854, 2000.

[17] Y. Tang, M. Tomizuka, G. Guerrero, and G. Montemayor, "Decentralized robust control of mechanical systems," *IEEE Trans. on Automatic Control*, vol. 45, no. 4, pp. 771–776, 2000.

[18] L. Bascetta and P. Rocco, "Revising the robust-control design for rigid robot manipulators," *IEEE Trans. on Robotics*, vol. 26, no. 1, pp. 180–187, Feb. 2010.

[19] J. Liu and X. Wang, *Advanced sliding mode control for mechanical systems*. Springer-Verlag Berlin Heidelberg, 2012.

[20] G. Bartolini, A. Pisano, E. Punta, and E. Usai, "A survey of applications of second-order sliding mode control to mechanical systems," *International Journal of control*, vol. 76, no. 9-10, pp. 875–892, 2003.

[21] G. Bartolini, A. Ferrara, and E. Usai, "Chattering avoidance by second-order sliding mode control," *IEEE Trans. Autom. Control*, vol. 43, no. 2, pp. 241–246, Feb 1998.

[22] T. Gonzalez, J. A. Moreno, and L. Fridman, "Variable gain super-twisting sliding mode control," *IEEE Trans. Autom. Control*, vol. 57, no. 8, pp. 2100–2105, Aug 2012.

[23] Wen-Hua Chen, D. J. Ballance, P. J. Gawthrop, and J. O'Reilly, "A nonlinear disturbance observer for robotic manipulators," *IEEE Trans. Ind. Electron.*, vol. 47, no. 4, pp. 932–938, Aug 2000.

[24] E. Sariyildiz, H. Sekiguchi, T. Nozaki, B. Ugurlu, and K. Ohnishi, "A stability analysis for the acceleration-based robust position control of robot manipulators via disturbance observer," *IEEE/ASME Trans. Mechatronics*, vol. 23, no. 5, pp. 2369–2378, Oct 2018.

[25] E. Sariyildiz, R. Oboe, and K. Ohnishi, "Disturbance observer-based robust control and its applications: 35th anniversary overview," *IEEE Trans. Ind. Electron.*, vol. 67, no. 3, pp. 2042–2053, 2020.

[26] S. Roy, S. B. Roy, and I. N. Kar, "Adaptive-Robust Control of EulerLagrange Systems With Linearly Parametrizable Uncertainty Bound," *IEEE Trans. Control Syst. Technol.*, vol. 26, no. 5, pp. 1842–1850, 2018.

[27] S. Roy, I. N. Kar, J. Lee, N. G. Tsagarakis, and D. G. Caldwell, "Adaptive-Robust Control of a Class of EL Systems With Parametric Variations Using Artificially Delayed Input and Position Feedback," *IEEE Trans. Control Syst. Technol.*, vol. 27, no. 2, pp. 603–615, 2019.

[28] S. Roy, S. Baldi, and L. M. Fridman, "On adaptive sliding mode control without a priori bounded uncertainty," *Automatica*, vol. 111, p. 108650, 2020.

[29] S. Gutman, "Uncertain dynamical systems–A Lyapunov min-max approach," *IEEE Trans. Autom. Control*, vol. 24, no. 3, pp. 437–443, 1979.

[30] J.-J. E. Slotine, "The robust control of robot manipulators," *The International Journal of Robotics Research*, vol. 4, no. 2, pp. 49–64, 1985.

[31] M. Corless and G. Leitmann, "Continuous state feedback guaranteeing uniform ultimate boundedness for uncertain dynamic systems," *IEEE Trans. Autom. Control*, vol. 26, no. 5, pp. 1139–1144, 1981.

[32] A. Jaritz and M. Spong, "An experimental comparison of robust control algorithms on a direct drive manipulator," *IEEE Trans. Control Syst. Technol.*, vol. 4, no. 6, pp. 627–640, 1996.

[33] B. Brogliato and C. C. de Wit, *Theory of Robot Control*. Springer-Verlag London, 1996, ch. Joint space control, pp. 59–114.

[34] S. Malan, M. Milanese, and M. Taragna, "Robust analysis and design of control systems using interval arithmetic," *Automatica*, vol. 33, no. 7, pp. 1363 – 1372, 1997.

[35] Y. Smagina and I. Brewer, "Using interval arithmetic for robust state feedback design," *Systems & Control Letters*, vol. 46, no. 3, pp. 187 – 194, 2002.

[36] I. Ferrer Mallorquí and J. Vehí, "Combining symbolic tools with interval analysis: An application to solve robust control problems," *American Journal of Computational Mathematics*, vol. 4, no. 3, pp. 183–196, 2014.

[37] S. Khadraoui, M. Rakotondrabe, and P. Lutz, "Interval modeling and robust control of piezoelectric microactuators," *IEEE Trans. Control Syst. Technol.*, vol. 20, no. 2, pp. 486–494, March 2012.

[38] A. Giusti and M. Althoff, "Ultimate robust performance control of rigid robot manipulators using interval arithmetic," in *Proc. American Control Conference*, 2016, pp. 2995–3001.

[39] F. Hisch, A. Giusti, and M. Althoff, "Robust control of continuum robots using interval arithmetic," *IFAC-PapersOnLine*, vol. 50, no. 1, pp. 5660 – 5665, 2017, 20th IFAC World Congress.

[40] R. E. Moore, R. B. Kearfott, and M. J. Cloud, *Introduction to Interval Analysis*. Philadelphia, PA, USA: Society for Industrial and Applied Mathematics, 2009.

[41] M. Althoff and D. Grebenyuk, "Implementation of interval arithmetic in CORA 2016," in *Proc. of the 3rd International Workshop on Applied Verification for Continuous and Hybrid Systems*, 2016, pp. 91–105.

[42] S. Rump, "INTLAB - INTerval LABoratory," in *Developments in Reliable Computing*, T. Csendes, Ed. Dordrecht: Kluwer Academic Publishers, 1999, pp. 77–104, http://www.ti3.tuhh.de/rump/.

[43] H. K. Khalil, *Nonlinear systems; 3rd ed.* Upper Saddle River, NJ: Prentice-Hall, 2002.

[44] A. Neumaier, *The Wrapping Effect, Ellipsoid Arithmetic, Stability and Confidence Regions*. Vienna: Springer Vienna, 1993, pp. 175–190.

[45] H. Roehm, J. Oehlerking, M. Woehrle, and M. Althoff, "Model Conformance for Cyber-Physical Systems: A Survey," *ACM Transactions on Cyber-Physical Systems*, vol. 3, no. 3, pp. 1–26, Aug 2019.

[46] ——, "Reachset Conformance Testing of Hybrid Automata," in *Hybrid Systems: Computation and Control*, 2016, vol. 29, pp. 277–286.

[47] S. B. Liu and M. Althoff, "Reachset Conformance of Forward Dynamic Models for the Formal Analysis of Robots," in *IEEE/RSJ Int. Conf. on Intelligent Robots and Systems*. IEEE, 2018, pp. 370–376.

[48] S. Boyd and L. Vandenberghe, *Convex Optimization*. Cambridge University Press, mar 2004, vol. 100, no. 471.

[49] R. Ortega and M. W. Spong, "Adaptive motion control of rigid robots: A tutorial," *Automatica*, vol. 25, no. 6, pp. 877–888, 1989.

[50] N. T. Nguyen, "Optimal control modification for robust adaptive control with large adaptive gain," *Systems & Control Letters*, vol. 61, no. 4, pp. 485–494, 2012.

[51] M. Althoff, A. Giusti, S. Liu, and A. Pereira, "Effortless creation of safe robots from modules through self-programming and self-verification," *Science Robotics*, vol. 4, no. 31, p. eaaw1924, 2019.
[52] A. Giusti and M. Althoff, "On-the-fly control design of modular robot manipulators," *IEEE Trans. Control Syst. Technol.*, vol. 26, no. 4, pp. 1484–1491, July 2018.
[53] A. Giusti and M. Althoff, "Efficient computation of interval-arithmetic-based robust controllers for rigid robots," in *Proc. First IEEE International Conference on Robotic Computing*, Apr. 2017, pp. 129–135.
[54] J. Luh, M. Walker, and R. Paul, "On-line computational scheme for mechanical manipulators," *ASME J. Dyn. Sys., Meas., Control*, vol. 102, pp. 468–474, 1980.
[55] A. De Luca and L. Ferrajoli, "A modified Newton-Euler method for dynamic computations in robot fault detection and control," in *Proc. IEEE Int. Conf. on Robotics and Automation*, 2009, pp. 3359–3364.
[56] A. Rausch and J. Oehlerking, "Report on Conformance Testing in the Development Process," Tech. Rep., 2018. [Online]. Available: https://cps-vo.org/node/59911
[57] M. Wagner, S. B. Liu, A. Giusti, and M. Althoff, "Interval-arithmetic-based trajectory scaling and collision detection for robots with uncertain dynamics," in *Proc. Second IEEE International Conference on Robotic Computing*. IEEE, 2018, pp. 41–48.

Andrea Giusti is researcher at Fraunhofer Italia Research, Italy. He received his Ph.D. degree in Robotics in 2018, from the Technical University of Munich (TUM), Germany. He received his Masters Degree in Mechatronic Engineering, summa cum laude, in 2013, and his Bachelors Degree in Telecommunications Engineering in 2010, both from University of Trento, Italy. His research interests include modeling and control of mechatronic systems, modular and reconfigurable robots, and human-robot collaboration.

Stefan B. Liu received the B.S. degree in mechatronics, and the M.S. degree in robotics from the Technical University of Munich (TUM), Germany, in 2015, and 2017, respectively. He is currently pursuing a Ph.D. degree at the Cyber-Physical Systems Group of the TUM Department of Informatics. His research interest includes formal methods in robotics, physical human-robot interaction, modeling and identification, and modular robots.

Matthias Althoff is Associate Professor in computer science at Technische Universität München, Germany. He received his Diploma Engineering Degree in Mechanical Engineering in 2005, and his Ph.D. in Electrical Engineering in 2010, both from Technische Universität München, Germany. From 2010 to 2012 he was a postdoctoral researcher at Carnegie Mellon University, Pittsburgh, USA, and from 2012 to 2013 an assistant professor at Technische Universität Ilmenau, Germany. His research interests include formal verification of continuous and hybrid systems, reachability analysis, planning algorithms, nonlinear control, robotics, automated vehicles, and power systems.